Progress In Electromagnetics Research, PIER 89, 1–10, 2009

EFFICIENT OPTIMIZATION AND REALIZATION OF A SHAPED-BEAM PLANAR ARRAY FOR VERY LARGE ARRAY APPLICATION

H. J. Zhou, B. H. Sun, J. F. Li, and Q. Z. Liu

National Key Laboratory of Antennas and Microwave Technology
Xidian University
Xi'an, Shaanxi 710071, China

Abstract—The optimization and simulated realization of planar 2-D antenna array with a flat-top shaped-beam pattern are proposed in this paper. The shaped-beam planar array can be used as an element of Very Large Array for the Deep Space Detection. A conventional genetic algorithm is chosen for the optimization. However, the synthesis of flat-top shaped-beam using a planar 2-D array is difficult because of the inherently large number of degrees of freedom involved in the algorithm (in generally, the amplitude and phase of each element must be determined). Therefore, a sub-array rotation method, which lies on the flat-top pattern synthesis itself, is proposed in this study to resolve the design problem. Besides, the proposed synthesis has taken the actual element patterns but identical and isotropic ones into account, which can reduce the error between computation and realization. A 8×8 (64)-element rectangular array is exampled, and the results of the optimized flat-top patterns are shown to illustrate the validity and high efficiency of the technique.

1. INTRODUCTION

In recent years, more and more spacecrafts are sent out to explore the solar system. The distances over which this communication takes place are extraordinarily large by Earth-based standards, and the power available for transmitting from the spacecraft is very low (typically 20 W or less). So, the signal arriving from a receding deep-space spacecraft becomes weaker and weaker. Then, the need arises for devising schemes to compensate for the reduction in signal-to-noise

Corresponding author: H. J. Zhou (zhjhere@163.com).

ratio (SNR). One remaining method for improving the effective SNR is to design flat-top pattern arrays acting as the elements to form a Very Large Array [1]. However, the synthesis of a planar 2-D antenna array with a specific radiation pattern, limited by several constraints, is a nonlinear optimization problem. Therefore, some heuristic algorithms, such as genetic algorithms (GA) will be necessary.

Genetic algorithm has garnered widespread use in the electromagnetic community because of its ability to solve complex multi-dimensional optimization problems with relative ease [2–4]. In antenna array pattern synthesis applications, the GA has been used extensively in the synthesis of 1-D linear antenna array patterns [5–9]. Its extension to 2-D planar arrays [10–12], although quite trivial conceptually, is not as trivial in practice, primarily due to the much large number of elements in planar 2-D arrays, which translates into a much large number of unknown parameters for the optimization algorithm. This increase in the number of degrees of freedom leads to a proportional increase in the dimensionality and complexity of the search space for the GA. To overcome this drawback, a parallel GA optimization tool for the synthesis is proposed in [13]. But, this tool requires the hardware equipments with high performance.

In this paper, a sub-array rotation method is presented during the optimization of a real-coded conventional GA, which can reduce the number of unknown parameters for the optimization. Besides, the proposed synthesis, being different from the most optimization in reported literatures, has taken the actual element patterns but identical and isotropic ones into account, which can reduce the error between computation and realization. In Section 2, the sub-array rotation method is presented and a simple mathematical model for the 2-D planar antenna array is also described. Examples and results illustrating the beam-forming capability of the proposed method are shown in Section 3. Section 4 gives the conclusion.

2. MATHEMATICAL MODEL OF THE PLANAR ARRAY AND SUB-ARRAY ROTATION METHOD

2.1. Sub-array Rotation Method

Since the radiation pattern of a 2-D planar array will be optimized, we begin with the general expression of the far filed of a $N \times N$-element planar antenna array, given by:

$$E(\theta, \varphi) = \sum_{n=1}^{N \times N} g_n(\theta, \varphi) \cdot a_n \exp\left[j\left(\bar{k} \cdot \bar{r}_n + \beta_n\right)\right] \tag{1}$$

where,

$$\overline{k} = k_0(\hat{x}\sin\theta\cos\varphi + \hat{y}\sin\theta\sin\varphi + \hat{z}\cos\theta) \text{ and } \overline{r}_n = \hat{x}x_n + \hat{y}y_n + \hat{z}z_n. \tag{2}$$

Here, $k_0 = 2\pi/\lambda$ is the free space wave-number, and (x_n, y_n, z_n) denotes the Cartesian coordinates for the nth radiating element of the array. The excitation of the nth element located at $\bar{r}_n$ is $a_n \exp(j\beta_n)$. The expression $g_n(\theta, \varphi)$ represents the radiation pattern of the nth element.

During the optimization, we choose to make use of a real encoding scheme, with a $2 \times N \times N$-gene chromosome consisting of the amplitude a_n and phase β_n for each of the $N \times N$ radiating element of a given antenna array. As mentioned before, the large number of degrees of freedom involved in the optimization will surely slow down the rapidity of convergence. To overcome this drawback, we present a sub-array rotation method, which lies on the flat-top shaped beam synthesis itself. Since the optimized radiation pattern of the planar array is flat-top shaped-beam and low peak side-lobe, the optimum result can be symmetrical about the x-axis and the y-axis. We may adjust the array configuration by the strong hand to make the pattern to be symmetrical. First, we construct the antenna array in the first quadrant of the Cartesian coordinates as a sub-array, whose dimension is $(N/2) \times (N/2)$, (N is even). And then, the arrays of other three quadrants are created by rotating the sub-array in the first quadrant in turn. Fig. 1 illustrate the sub-array with $(N/2) \times (N/2)$ $(N = 8)$ elements and the new configuration of the $N \times N$-element array with an equal inter-element spacing d. Note that, the elements of the total array are arranged in the same polarization, it is the excitation of the array elements that are rotated.

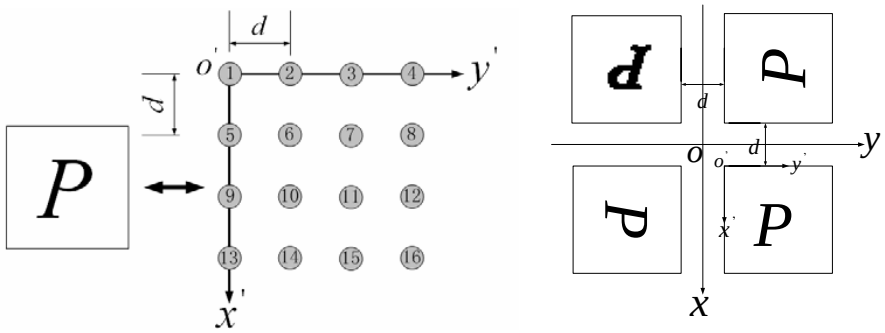

(a) Sub-array (b) Total array

Figure 1. Configuration of the $N \times N$-element rectangular array.

In this case, we can rewrite the array pattern of the sub-array in the first quadrant. It can be expressed as:

$$SUB\_EA(\theta,\varphi) = \sum_{n=1}^{\frac{N}{2}\times\frac{N}{2}} g_n(\theta,\varphi)\cdot a_n \exp\left[j\left(\bar{k}\cdot\bar{r}_n+\beta_n\right)\right], \quad \theta\in[0,\pi/2],\quad \varphi\in[0,2\pi] \tag{3}$$

Since the arrays in the other three quadrants are created by rotating the sub-array, the radiation patterns of the total array in four quadrants should be symmetrical. So, we can just discuss the far field radiation pattern in the first quadrant produced by the total array. Fortunately, the radiation patterns in the first quadrant which resulting from the arrays in each quadrant can be expressed respectively by (3):

$$\begin{array}{l} E1\left(\theta',\varphi'\right) = SUB\_EA(\theta',\varphi')\,; \\ E2\left(\theta',\varphi'\right) = SUB\_EA(\theta',\varphi'+3\pi/2)\,; \\ E3\left(\theta',\varphi'\right) = SUB\_EA(\theta',\varphi'+\pi)\,; \\ E4\left(\theta',\varphi'\right) = SUB\_EA(\theta',\varphi'+\pi/2)\,; \end{array} \quad \theta'\in[0,\pi/2],\ \varphi'\in[0,\pi/2] \tag{4}$$

Note that, all the array factor patterns in (3) and (4) are calculated in the Cartesian coordinates $x'o'y'$ illustrated in Fig. 1(a). When we calculate the far field of the total array shown in Fig. 1(b), the phase difference attributed to wave path difference between the reference-points of the sub-array in each quadrant must be taken into account. So, the far field radiation pattern of the $N\times N$-element array can be written as:

$$\begin{aligned} EE\left(\theta',\varphi'\right) = {} & \exp\left[\frac{jkd}{2}\left(\sin\theta'\cos\varphi'+\sin\theta'\sin\varphi'\right)\right]\cdot E1\left(\theta',\varphi'\right) \\ & + \exp\left[\frac{jkd}{2}\left(-\sin\theta'\cos\varphi'+\sin\theta'\sin\varphi'\right)\right]\cdot E2\left(\theta',\varphi'\right) \\ & + \exp\left[\frac{jkd}{2}\left(-\sin\theta'\cos\varphi'-\sin\theta'\sin\varphi'\right)\right]\cdot E3\left(\theta',\varphi'\right) \\ & + \exp\left[\frac{jkd}{2}\left(\sin\theta'\cos\varphi'-\sin\theta'\sin\varphi'\right)\right]\cdot E4\left(\theta',\varphi'\right) \end{aligned} \tag{5}$$

Obviously, in this case, the total length of the gene chromosome consisting of the amplitude a_n and phase β_n for each element of the sub-array has become $2\times\frac{N}{2}\times\frac{N}{2}=\frac{N\times N}{2}$, reducing to the quarter of previous one. Besides, the far fields in each quadrant are same thanks to the rotational symmetry of the array. As a result, we can only sample the electric field points in the first quadrant of the total array. Without question, the new optimization process consequently turns to be more effective.

2.2. 3-D Element Pattern Reconstructed

Being different from the most array synthesis reported in printed literatures, the proposed optimization has taken the array element factor into account. Usually, we can only get the two principal cuts of the 3-D radiation pattern. Thus, an adequate estimate of the 3-D antenna radiation solid should be employed. In this paper, we choose a technique presented by GVAS [14] for the 3-D pattern reconstruction from only the azimuth and elevation cuts. Note thatwhen axially symmetric (omni) patterns are reconstructed by GVAS, the approximation errors is zero. Otherwise, there will be a slight acceptable error between the computation and reconstruction. The azimuth pattern is actually the planar cut at $\theta = \pi/2$ while the vertical pattern is the cut at $\varphi = 0$. Example decimal gain patterns are depicted as $hor(\varphi)$ and $vert(\theta)$, respectively. Also, we define as G_H and G_V their corresponding logarithmic counterparts (in decibels), i.e., $G_H(\varphi) = 10 \cdot \log[hor(\varphi)]$ and $G_V(\theta) = 10 \cdot \log[vert(\theta)]$. At an arbitrary point (φ, θ), the approximated antenna gain G is calculated by weighting the horizontal/vertical samples (at the point of interest), according to the following formula:

$$G(\varphi,\theta) = \frac{G_H(\varphi)\cdot w_1 + G_V(\theta)\cdot w_2}{\sqrt[2]{w_1^2 + w_2^2}}$$

$$w_1(\varphi,\theta) = vert(\theta)\cdot[1 - hor(\varphi)]; \quad w_2(\varphi,\theta) = hor(\varphi)\cdot[1 - vert(\theta)].$$

If $w_1^2 + w_2^2 = 0$, then $G(\varphi,\theta) = G_H(\varphi) + G_v(\theta)$.

Figure 2 depicts the comparison of the patterns in four cuts ($\varphi = 0^\circ, 45^\circ, 90^\circ, 135^\circ$) obtained from the 3-D reconstruction technique (GVAS) and Ansoft high-frequency structure simulation (HFSS), respectively. Due to the asymmetry of the patterns, there exists slight approximation error between the computation and reconstruction. However, it can be seen that the approximation error is close to zero in $-30^\circ \sim 30^\circ$ region.

2.3. Shaped-beam Optimization

The fitness function for this study is defined in the following manner. For each field sample point in shaped-beam regions, the relative error is the difference between the actual power level and that of the desired pattern over M total sample points:

$$e_m = S_{actual}(\theta_m, \varphi_m) - S_{desired}(\theta_m, \varphi_m), \quad m = 1, 2, \ldots, M \qquad (6)$$

where S denotes the power density pattern of the array. A least mean-square measure is used to represent the overall pattern error as:

$$EMA = \left(\frac{1}{M} \sum_{m=1}^{M} |e_m|^2 \right)^{\frac{1}{2}} \tag{7}$$

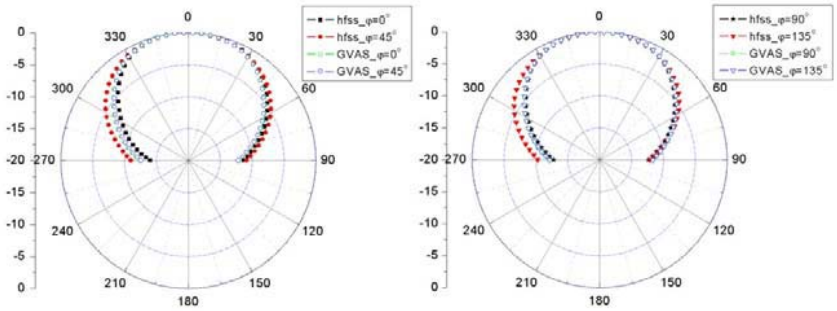

(a) Patterns of element 1 in Figure 1(a)

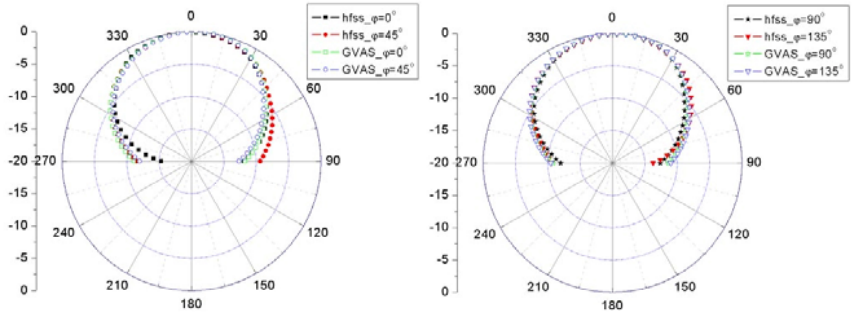

(b) Patterns of element 4 in Figure 1(a)

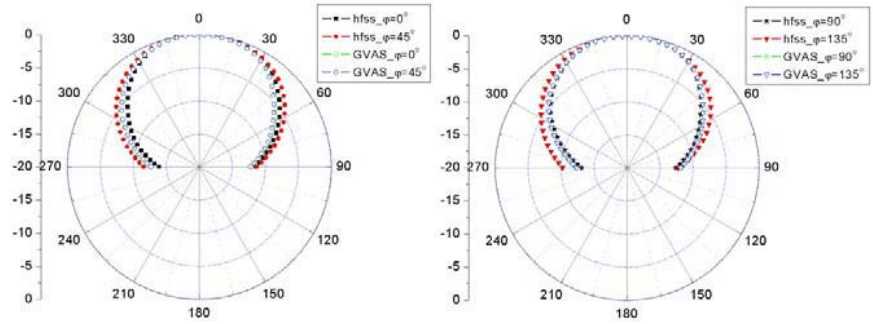

(c) Patterns of element 11 in Figure 1(a)

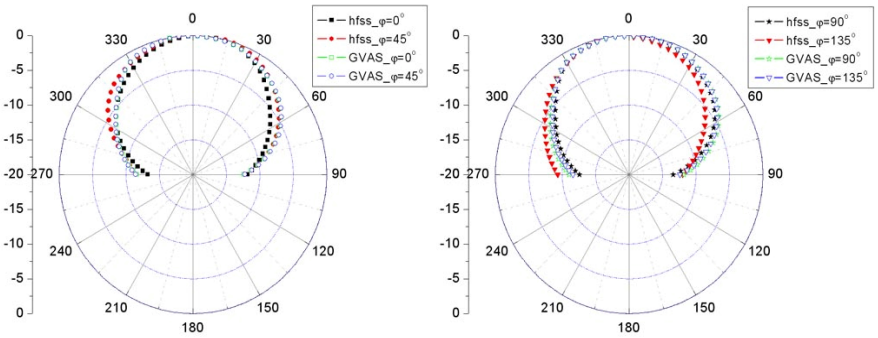

(d) Patterns of element 13 in Figure 1(a)

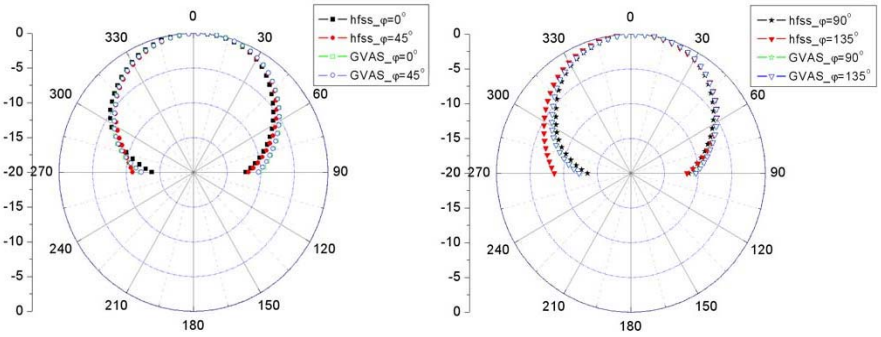

(e) Patterns of element 16 in Figure 1(a)

Figure 2. Comparison of the patterns obtained from the 3-D reconstruction technique (GVAS) and ansoft high-frequency structure simulation (HFSS).

On the other hand, the peak side-lobe level (PSLL) of the array pattern must be considered. The PSLL can easily be searched out in side-lobe regions and the difference between the computational PSLL and the desired can be expressed as:

$$EMB = PSLL_{actual} - PSLL_{desired} \tag{8}$$

Then, the hybrid difference is given by:

$$\begin{aligned} EM &= w \times EMA + EMB \\ &= w \times \left(\frac{1}{M} \sum_{m=1}^{M} |e_m|^2 \right)^{\frac{1}{2}} + (PSLL_{actual} - PSLL_{desired}) \end{aligned} \tag{9}$$

where w is a weighting parameter that can be used to emphasize the shaped-beam regions. In order to assign the fitness value within the normalized range [0, 1], the fitness function can be defined as:

$$fitness = \frac{EM}{1 + EM} \tag{10}$$

3. RESULTS AND DISCUSSION

Since the optimized array acting as a element of the Very Large Array for Deep Space Detection is a flat-top shaped-beam array, an 8×8-element array is chosen to validate the efficiency and accuracy of the proposed method. Considering the complexity in realizing the feeding network of the array, the amplitude and phase of the element excitation are limited in $[1, 8]$ and $[0, 360°]$, respectively. The optimized pattern with a flat-top main beam of about 20° and a peak side-lobe level of -15 dB is obtained by GA completed with a MATLAB program. Also, the proposed array is also simulated by Ansoft high-frequency structure simulation (HFSS) for comparison. Fig. 3 depicts the normalized flat-top patterns in six principal planes ($\varphi = 0°, 30°, 60°, 90°, 120°, 150°$) obtained by GA optimization and simulation using HFSS. It is observed that the maximal ripple in the shaped-beam region covering $-10° \sim 10°$ is about 0.96 dB and the PSLL is -15 dB. The difference between the computation and simulation in side-lobe region may be due to approximation errors from 3-D patterns reconstruction. The element excitation distribution for the pattern obtained by optimization of both amplitude and phase is depicted in Fig. 4.

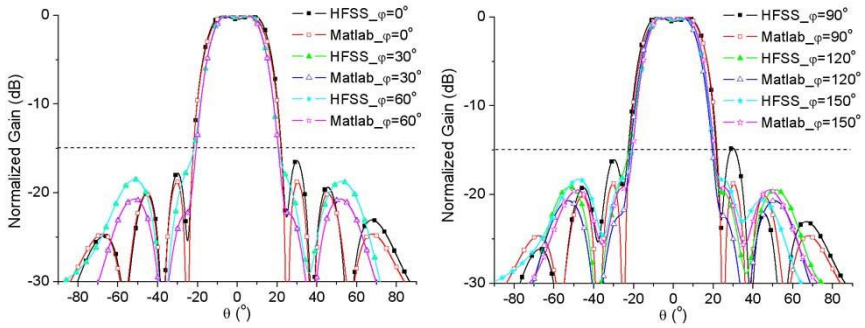

Figure 3. Normalized flat-top patterns obtained from computation and HFSS.

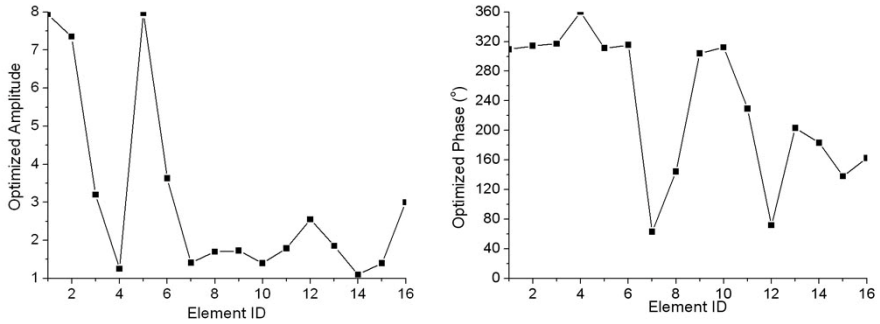

Figure 4. Optimized element excitation distribution of sub array for the flat-top pattern.

4. CONCLUSIONS

In this paper, we presented the optimization of a flat-top pattern of the planar 2-D array antenna, which is used to be an element of Very Large Array for the deep space detection. A sub-array rotation method, which lies on the flat-top pattern synthesis itself, has been proposed for enhancing the optimization efficiency. Besides, the actual element patterns which are obtained from a reported technique have been taken into account in array synthesis for reducing the error between computation and realization. An 8×8-element array has been employed, and the results of the optimized flat-top pattern are shown to illustrate the high efficiency and validity of the proposed method.

REFERENCES

1. Rogstad, D. H., A. Mileant, and T. T. Pham, *Antenna Arraying Techniques in the Deep Space Network*, Jet Propulsion Laboratory, California, United States, January 2003.
2. Rahmat-Samii, Y. and E. Michielssen, *Electromagnetic Optimization by Genetic Algorithms*, Wiley, New York, 1999.
3. Weile, D. S. and E. Michielssen, "Genetic algorithm optimization applied to electromagnetics: A review," *IEEE Trans. on Antennas and Propag.*, Vol. 45, 343–353, March 1997.
4. Lu, Y. Q., "Optimization of broadband top-load antenna using micro-genetic algorithm," *Journal of Electromagnetic Waves and Applications*, Vol. 20, No. 6, 793–801, 2006.
5. Rao, K. S., "A template for shaped-beam satellite antenna

patterns," *IEEE Trans. on Antennas and Propag.*, Vol. 36, 1633–1637, November 1988.

6. Buckley, M. J., "Synthesis of shaped beam antenna patterns using implicitly constrained current elements," *IEEE Trans. on Antennas and Propag.*, Vol. 44, 192–197, February 1996.
7. Marcano, D. and F. Duran, "Synthesis of antenna arrays using genetic algorithms," *IEEE Antennas and Propagation Mag.*, Vol. 42, 12–19, June 2000.
8. Soltankarimi, F., J. Nourinia, and C. Ghobadi, "Side lobe level optimization in phased array antennas using genetic algorithm," *Proc. Int. Symp. on Antennas and Propagation*, 389–393, June 2004.
9. Lei, J., G. Fu, L. Yang, and D. M. Fu, "Multi-objective optimization design of the YAGI-UDA antenna with an X-shape driven dipole," *Journal of Electromagnetic Waves and Applications*, Vol. 21, No. 7, 963–972, 2007.
10. Hwang, R. B. and T. C. Pu, "A planar shaped-beam antenna for indoor wireless lan access points," *IEEE Trans. on Antennas and Propag.*, Vol. 55, 1871–1878, June 2007.
11. Cui, B., J. Zhang, and X. W. Sun, "Single layer micro-strip antenna arrays applied in millimeter-wave radar," *Journal of Electromagnetic Waves and Applications*, Vol. 22, No. 1, 3–15, 2008.
12. Donelli, M., S. Caorsi, F. de Natale, D. Franceschini, and A. Massa, "Versatile enhanced genetic algorithm for planar array design," *Journal of Electromagnetic Waves and Applications*, Vol. 18, No. 11, 1533–1548, 2004.
13. Villegas, F. J., "Parallel genetic-algorithm optimization of shaped beam coverage areas using planar 2-D phased arrays," *IEEE Trans. on Antennas and Propag.*, Vol. 55, 1745–1753, June 2007.
14. Vasiliadis, T. G., A. G. Dimitriou, and G. D. Sergiadis, "A novel technique for the approximation of 3-D antenna radiation patterns," *IEEE Trans. on Antennas and Propag.*, Vol. 53, 2212–2219, July 2005.